

**Manuscript version: Published Version**

The version presented in WRAP is the published version (Version of Record).

**Persistent WRAP URL:**

<http://wrap.warwick.ac.uk/172207>

**How to cite:**

The repository item page linked to above, will contain details on accessing citation guidance from the publisher.

**Copyright and reuse:**

The Warwick Research Archive Portal (WRAP) makes this work by researchers of the University of Warwick available open access under the following conditions.

Copyright © and all moral rights to the version of the paper presented here belong to the individual author(s) and/or other copyright owners. To the extent reasonable and practicable the material made available in WRAP has been checked for eligibility before being made available.

Copies of full items can be used for personal research or study, educational, or not-for-profit purposes without prior permission or charge. Provided that the authors, title and full bibliographic details are credited, a hyperlink and/or URL is given for the original metadata page and the content is not changed in any way.

**Publisher's statement:**

Please refer to the repository item page, publisher's statement section, for further information.

For more information, please contact the WRAP Team at: [wrap@warwick.ac.uk](mailto:wrap@warwick.ac.uk)

# Common envelope evolution and triple dynamics as potential pathways to form the inner white dwarf + brown dwarf binary of the triple star system Gaia 0007–1605

Felipe Lagos,<sup>1</sup>★ Monica Zorotovic,<sup>2</sup> Matthias R. Schreiber<sup>3,4</sup> and B. T. Gänsicke<sup>1,5</sup> 

<sup>1</sup>Department of Physics, University of Warwick, Gibbet Hill, Coventry CV4 7AL, UK

<sup>2</sup>Instituto de Física y Astronomía, Universidad de Valparaíso, Avenida Gran Bretaña 1111, Valparaíso, Chile

<sup>3</sup>Departamento de Física, Universidad Técnica Federico Santa María, Avenida España 1680, Valparaíso, Chile

<sup>4</sup>Millennium Nucleus for Planet Formation, NPF, Valparaíso 2340000, Chile

<sup>5</sup>Centre for Exoplanets and Habitability, University of Warwick, Coventry CV4 7AL, UK

Accepted 2022 December 7. Received 2022 November 18; in original form 2022 July 16

## ABSTRACT

The recently discovered system Gaia 0007–1605 consisting of a white dwarf (WD) with a close brown dwarf companion and a distant WD tertiary very much resembles the triple system containing the first transiting planet candidate around a WD ever discovered: WD 1856+534. We have previously argued that the inner binary in WD 1856+534 most likely formed through common envelope evolution but triple star dynamics represent an alternative scenario. Here, we analyse different formation scenarios for Gaia 0007–1605. We reconstructed the potential common envelope evolution of the system and found that assuming standard parameters for the energy budget provides a reasonable solution. In agreement with other close white dwarf + brown dwarf binaries, and in contrast to WD 1856+534, no energy sources other than orbital energy during common envelope evolution are required to understand the current configuration of the system. In addition, using analytical prescriptions for triple dynamics, we show that Von Zeipel–Lidov–Kozai oscillations might have triggered tidal migration due to high-eccentricity incursions ( $e \gtrsim 0.997$ ). We conclude that the inner binary in Gaia 0007–1605, as its sibling WD 1856+534, formed either through common envelope evolution, triple dynamics, or a combination of both mechanisms.

**Key words:** binaries: close; brown dwarfs; white dwarfs.

## 1 INTRODUCTION

White dwarfs (WDs) that are members of close binaries<sup>1</sup> are important in a wide range of astrophysical contexts including studies of Type Ia supernovae or the detection of gravitational waves. The classical formation scenario for close binary stars containing a WD is common envelope evolution (Paczynski 1976).

Common envelope evolution is an inherently complicated process and it has so far turned out to be impossible to cover the large range of spatial and temporal scales in hydrodynamic simulations (Ivanova et al. 2013). To compare observations and model predictions, proper simulations of the process are therefore often replaced by a parametrized energy equation relating the binding energy of the envelope and the change in orbital energy of the binary.

Observed samples of close WD binaries with main-sequence star companions can be used to constrain the energy budget during common envelope evolution. In the vast majority of cases, observed populations can be understood using a small common envelope efficiency and without assuming contributions from additional energy sources such as recombination energy. This finding holds for post

common envelope binaries with M-dwarf (Zorotovic et al. 2010), substellar (Zorotovic & Schreiber 2022), and sun-like (Hernandez et al. 2021, 2022a, b) companions.

However, the general success of the common envelope scenario in explaining the observed populations of close binaries does not exclude the existence of alternative formation scenarios of close WD binaries. Recently, Lagos et al. (2022) showed that the period distribution of WDs with close G-type companions can be explained if systems with periods of months to years form through stable but non-conservative mass transfer (see also Masuda et al. 2019). The situation is similar for the observed population of double WDs, i.e. their characteristics can be best explained by considering the possibility of common envelope evolution and stable non-conservative mass transfer (e.g. Nelemans et al. 2000; Webbink 2008; Woods et al. 2012).

Another alternative for forming close WD binaries is triple dynamics. The inner binary of a hierarchical triple system may exchange angular momentum with the orbit of the distant tertiary through the so-called Von Zeipel–Lidov–Kozai (ZLK) mechanism (Von Zeipel 1910; Kozai 1962; Lidov 1962), which may generate large eccentricities and subsequent tidal decay in the inner binary. ZLK oscillations have been used to explain a large variety of phenomena, including the formation of hot Jupiters (e.g. Wu & Murray 2003; Naoz et al. 2011; Petrovich 2015) or blue stragglers (e.g. Perets & Fabrycky 2009) and may even result in the merger of double WD binaries (e.g. Thompson 2011).

\* E-mail: [felipe.lagos.vilches@gmail.com](mailto:felipe.lagos.vilches@gmail.com)

<sup>1</sup>Through the paper, we use the term ‘close binary’ to refer to binaries with orbital periods up to hundred of days.

**Table 1.** Stellar parameters and ages for Gaia0007–1605 reported by Rebassa-Mansergas et al. (2022). Values with ‘\*’ require further confirmation. In particular, the total age of the systems is based on the sum of the cooling age of the outer WD and its main-sequence progenitor lifetime, which in turn depends on the initial-to-final mass relation. However, the latter is not well defined in the mass range of the outer WDs. The mass of the BD is based on its  $L3 \pm 1$  spectral type.

Parameter	Inner WD	Brown dwarf	Outer WD
Mass ( $M_{\odot}$ )	$0.54 \pm 0.01$	0.07*	$0.56 \pm 0.05$
Orbital period (d)	$1.0446 \pm 0.0015$	$1.0446 \pm 0.0015$	–
Cooling time (Gyr)	$0.360 \pm 0.002$	–	$8.2 \pm 0.2$
Total age (Gyr)	$\simeq 10^*$	$\simeq 10^*$	$\simeq 10^*$
Projected separation (au)	–	–	1673.11

So far, however, the formation of close WD binaries through ZLK oscillations remains hypothetical. To the best of our knowledge, a triple system where an inner binary containing a WD has formed most likely through triple dynamics and tidal migration has not yet been identified. The perhaps most promising candidate known is the transiting gas giant planet around WD 1856+534 that is part of a hierarchical triple system (Vanderburg et al. 2020). While ZLK oscillations could in principle be responsible for the currently observed configuration (e.g. Muñoz & Petrovich 2020; O’Connor, Liu & Lai 2021; Stephan, Naoz & Gaudi 2021), it has also been shown that common evolution can explain its tight orbit (Chamandy et al. 2021; Lagos et al. 2021; Merlov, Bear & Soker 2021). Measuring the mass of the transiting planet could constrain the evolutionary history of the system. While common envelope evolution is disfavoured for masses below  $5 M_{\text{jup}}$ , ZLK oscillations also cover lower masses being the most likely scenario below  $3 M_{\text{jup}}$ . Unfortunately, according to the lower limits derived from transmission spectroscopy that appear in the literature ( $0.84$  and  $2.4 M_{\text{jup}}$  at there  $2\sigma$  level, Alonso et al. 2021; Xu et al. 2021) both scenarios remain plausible.

Recently, a system very similar to WD 1856+534 has been found and characterized by Rebassa-Mansergas et al. (2022). They showed that the infrared excess of the WD Gaia0007–1605 is caused by a brown dwarf (BD) companion and using spectral fits combined with *Gaia* photometry they convincingly constrained most of the parameters of both components, with exception of the BD mass and the total age of the system (see Table 1). El-Badry, Rix & Heintz (2021) and Rebassa-Mansergas et al. (2021) furthermore revealed that the close WD + BD binary is in fact the inner binary of a hierarchical triple system by discovering a common proper motion WD companion. The distant WD was characterized based on photometry only and the estimated parameters – although in agreement with previous rough estimates (Gentile Fusillo et al. 2021) – are therefore less certain. The total age of the system derived from the parameters of the tertiary is  $\sim 10$  Gyr, which is in agreement with the likely membership of the system to the Galactic disc.

We here present an investigation of the potential evolutionary history of Gaia0007–1605 using standard prescriptions for common envelope evolution and analytical approximations describing possible ZLK oscillations. We find that common envelope evolution represents a natural explanation for the current configuration and that the formation of Gaia0007–1605 can be reproduced with a small common envelope efficiency, such as virtually all post common envelope binaries. Tidal migration induced by ZLK oscillations also represents a plausible scenario as long as the BD survives the post-main-sequence evolution of its host star and its eccentricity reaches values greater than  $\approx 0.997$ .

## 2 RECONSTRUCTING THE EVOLUTION OF THE INNER BINARY WITH COMMON ENVELOPE EVOLUTION

We reconstructed the evolutionary history of the inner WD + BD binary in Gaia0007–1605 assuming that it evolved to its current short orbital period during a common envelope phase and without influence of the distant companion on the orbital period decrease. We used the same method recently described in Zorotovic & Schreiber (2022) for a sample of well characterized close WD + BD binaries. In summary, we first calculated the period that the system had immediately after ejecting the envelope based on the WD cooling age and angular momentum loss in the post common envelope phase through gravitational radiation only (Schreiber & Gänsicke 2003). We then searched for possible progenitors of the WD within a grid calculated with the single-star-evolution (SSE) code from Hurley, Pols & Tout (2000) for solar metallicity, and reconstructed the common envelope phase using Roche-geometry and the *energy formalism* developed by Webbink (1984), assuming that no energy sources other than orbital and thermal energy contributed to unbinding the envelope (for more details, see Zorotovic & Schreiber 2022).

In Fig. 1, we present the results for the estimated total age of the system (top panel), initial mass of the progenitor of the WD ( $M_{\text{prog,wd}}$ , middle panel), and orbital period at the onset of the common envelope phase ( $P_{\text{CE,in}}$ , bottom), as a function of the common envelope efficiency  $\alpha_{\text{CE}}$  (i.e. the fraction of the change in orbital energy that is used to unbind the envelope). The darker results correspond to solutions assuming a WD mass within the error given by Rebassa-Mansergas et al. (2022, i.e.  $0.01 M_{\odot}$ ), while the results marked using light grey allow the WD mass to vary within a range of  $\pm 0.05 M_{\odot}$ . In all cases, the WD progenitor filled its Roche Lobe on the asymptotic giant branch (AGB), meaning the WD is composed of carbon and oxygen. Assuming that the WD mass is accurate within the small error given by Rebassa-Mansergas et al. (2022), we derive a maximum age of  $\sim 6$  Gyr for the system, which is not consistent with the large age the authors derived based on the distant WD companion. In order to obtain a larger total age of  $\sim 10$  Gyr, the WD mass needs to be slightly smaller than estimated by Rebassa-Mansergas et al. (2021,  $\sim 0.51 M_{\odot}$ ), implying it descends from a low-mass progenitor ( $\lesssim 1.1 M_{\odot}$ ) with a larger main-sequence lifetime. Also, a low-mass progenitor would have less mass in the envelope at the onset of the common envelope phase, which allows the common envelope efficiency to be smaller, i.e.  $\alpha_{\text{CE}} \sim 0.2$ – $0.4$ , consistent with the range of  $\alpha_{\text{CE}}$  derived for the sample of close WD + BD systems with accurate parameters (Zorotovic & Schreiber 2022).

## 3 POSSIBLE IMPACT OF TRIPLE DYNAMICS ON THE EVOLUTION

Given that the close inner WD + BD binary is part of a hierarchical triple, it might in principle be possible that ZLK oscillations had an impact on the formation of the close binary. If ZLK oscillations were present after the formation of the inner WD, one cannot a priori exclude that the inner binary perhaps did not form through common envelope evolution but that instead ZLK oscillations generated large eccentricities and subsequent tidal decay, producing the short orbital period of the WD + BD inner binary we observe today.

In what follows, we use the methodology developed by Muñoz & Petrovich (2020) to evaluate whether the formation of the close WD + BD binary can be understood by inward migration due to ZLK oscillations coupled with tidal friction after the formation of the inner white WD (henceforth the WD/BD + WD phase).

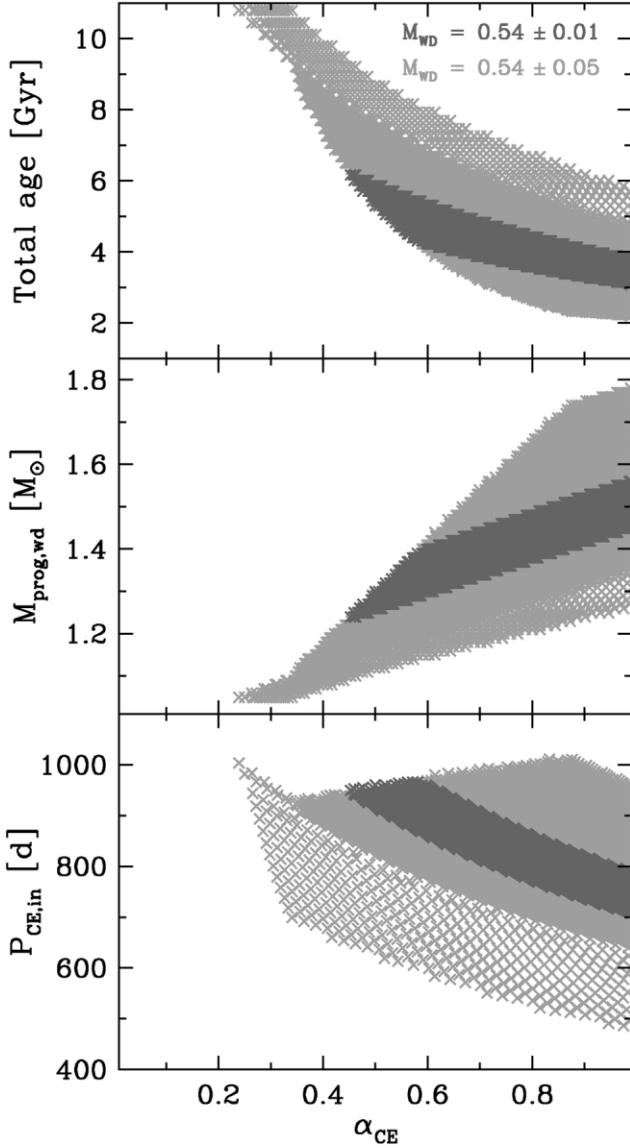


**Figure 1.** Total age of the system (*top*), initial mass of the progenitor of the WD (*middle*), and orbital period at the onset of the common envelope phase (*bottom*), as a function of the common envelope efficiency  $\alpha_{\text{CE}}$ , for the possible progenitors of the inner WD in our reconstruction.

### 3.1 Constraints for migration during the WD/BD + WD phase

After the formation of the second (inner) WD, migration of the BD is achieved if the inner eccentricity during ZLK oscillations is above a critical value  $e_{\text{mig}}$  required for tidal migration, but below  $e_{\text{dis}}$  to avoid tidal disruption. Both  $e_{\text{mig}}$  and  $e_{\text{dis}}$  can be obtained analytically as

$$e_{\text{mig}} = 1 - 1.96 \left( \frac{k_{2,\text{BD}} \Delta t_L T}{P_{\text{BD}}^2} \frac{M_{\text{WD,inner}}}{M_{\text{BD}}} \frac{R_{\text{BD}}^5}{a_{\text{BD}}^5} \right)^{1/7} \quad (1)$$

and

$$e_{\text{dis}} = 1 - \eta_{\text{dis}} \frac{R_{\text{BD}}}{a_{\text{BD}}} \left( \frac{M_{\text{WD,inner}}}{M_{\text{BD}}} \right)^{1/3} \quad (2)$$

(equations 9 and 10 of Muñoz & Petrovich 2020). Here,  $M_{\text{BD}}$ ,  $R_{\text{BD}}$ ,  $k_{2,\text{BD}}$ ,  $a_{\text{BD}}$ , and  $P_{\text{BD}}$  are the mass, radius, potential Love number of degree 2, semimajor axis, and orbital period of the BD, respectively.  $\Delta t_L$  is the lag time,  $T$  is the time interval in which the migration

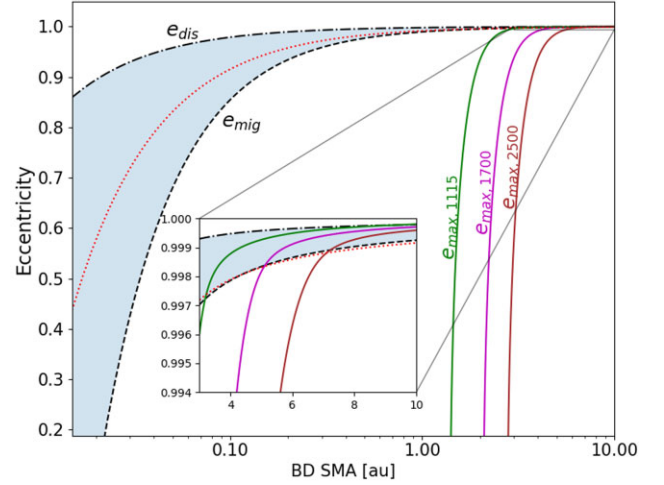


**Figure 2.** Eccentricity window (filled area) in which migration would occur during the WD/BD + WD phase as function of the semimajor axis of the BD. The boundaries of this window are set by equations 1 (dashed line) and 2 (dash-dotted line). The maximum eccentricity attained by the BD under the perpendicular TPQ approximation (i.e. solution of equation 4) as function of the BD semimajor axis and taking  $a_{\text{WD,outer}} = 1115, 1700,$  and  $2500$  au (green, magenta, and brown lines, respectively). The eccentricity required for the BD to reach its current orbital period (semimajor axis) after successful migration is given by the red dotted line, which has been calculated using equation (8).

occurs, and  $\eta_{\text{dis}} = 2.7$  is a numerical factor to estimate the minimum orbital separation at which tidal disruption will occur (Guillochon, Ramirez-Ruiz & Lin 2011).

For the inner WD, we assume a progenitor of  $1.07 M_{\odot}$ , which ends up as a WD with  $M_{\text{WD,inner}} \approx 0.52 M_{\odot}$  after  $\approx 9.7$  Gyr according to the SSE stellar evolution code (Hurley et al. 2000). In the same way, we assume for the outer WD a progenitor of  $1.7 M_{\odot}$  that formed a  $0.6 M_{\odot}$  WD after  $\approx 2.1$  Gyr. For the BD mass, we use the value estimated by Rebassa-Mansergas et al. (2022) of  $0.07 M_{\odot}$  while its radius is assumed to be  $0.086 R_{\odot}$  based on the BD isochrones<sup>2</sup> of Baraffe et al. (2003).  $k_{2,\text{BD}}$  is set to 0.286 (Heller et al. 2010),  $\Delta t_L = 1$  s (i.e. 10 times the Jupiter lag time), and  $T = 0.3$  Gyr assuming a total age of 10 Gyr. Fig. 2 shows the range of eccentricities  $e_{\text{mig}} < e < e_{\text{dis}}$  that allow for migration as function of  $a_{\text{BD}}$ . The migration windows become very narrow at  $a_{\text{BD}} \approx 1$  au, ranging from  $0.988 \approx e \lesssim 0.997$ .

During ZLK oscillations, extremely high eccentricities ( $e \approx 1$ ) can be achieved at the octupolar level of approximation. The importance of this regime is usually measured by

$$\epsilon_{\text{oct}} = \left( \frac{M_{\text{WD,inner}} - M_{\text{BD}}}{M_{\text{WD,inner}} + M_{\text{BD}}} \right) \left( \frac{a_{\text{BD}}}{a_{\text{outer}}} \right) \frac{e_{\text{outer}}}{1 - e_{\text{outer}}^2}, \quad (3)$$

where  $a_{\text{outer}}$  and  $e_{\text{outer}}$  are the semimajor axis and eccentricity of the tertiary companion. In general, it is assumed that the octupole regime plays an important role in the evolution of the system when  $\epsilon_{\text{oct}} \gtrsim 0.001$ . Taking a conservative value of 1700 au for  $a_{\text{outer}}$  (based on the projected separation of  $\approx 1673$  au between both WDs) and  $e_{\text{outer}} = 0.5$ , the octupole regime in Gaia 0007–1605 becomes important when  $a_{\text{BD}} \gtrsim 3$  au.

To estimate the maximum eccentricity  $e_{\text{max}}$  attained by the inner binary in the octupolar regime, we use equation (7) of Muñoz &

<sup>2</sup>[http://perso.ens-lyon.fr/isabelle.baraffe/COND03\\_models](http://perso.ens-lyon.fr/isabelle.baraffe/COND03_models)

Petrovich (2020), which is derived from the perpendicular test particle quadrupole (TPQ) approximation (Liu, Muñoz & Lai 2015; Naoz 2016) and assuming an initial circular inner orbit

$$0 = \frac{9}{8}e_{\max}^2 - \xi_{\text{GR}} \left( \frac{1}{(1 - e_{\max}^2)^{1/2}} - 1 \right) - \frac{\xi_{\text{tide}}}{15} \left( \frac{1 + 3e_{\max}^2 + \frac{3}{8}e_{\max}^4}{(1 - e_{\max}^2)^{9/2}} - 1 \right), \quad (4)$$

where

$$\xi_{\text{GR}} = \frac{3GM_{\text{WD,inner}}^2 a_{\text{outer}}^3 (1 - e_{\text{outer}}^2)^{3/2}}{a_{\text{BD}}^4 c^2 M_{\text{WD,outer}}} \quad (5)$$

and

$$\xi_{\text{tide}} = \frac{15M_{\text{WD,inner}}^2 a_{\text{outer}}^3 (1 - e_{\text{outer}}^2)^{3/2} k_{2,\text{BD}}}{a_{\text{BD}}^8 M_{\text{BD}} M_{\text{WD,outer}}} \quad (6)$$

are terms that represent the strength of general relativistic precession and tides relative to the quadrupolar potential of the triple system, with  $c$  being the speed of light. Solutions of equation (4) for the current configuration of the system are shown in Fig. 2. The value of  $e_{\max}$  (magenta line) reaches the migration window when  $a_{\text{BD}} \gtrsim 5.11$  au. The eccentricities for migration correspond to a small range of rather extreme values ( $e_{\text{mig}} = 0.9984 \lesssim e_{\max} \lesssim e_{\text{dis}} = 0.9998$ ).

The range of mutual inclinations [ $90^\circ - \Delta i$ ,  $90^\circ + \Delta i$ ] in which  $e_{\max}$  is attained can be estimated by

$$\Delta i = 2.9^\circ \left( \frac{\epsilon_{\text{oct}}}{10^{-3}} \right)^{1/2} \quad (7)$$

(equation 6 of Muñoz & Petrovich 2020). For a BD located at 5.11 au prior to migration,  $\Delta i \approx 3.6^\circ$ . If the mutual inclination is taken from an isotropic distribution (i.e. uniform in  $\cos i$ ), then the probability of Gaia 0007–1605 being in the inclination window required for migration is  $\approx 6$  per cent. It is worth mentioning that the value of  $\Delta i$  can be increased by assuming a larger inner semimajor axis but at the expense of reducing the eccentricity window for migration (unless the planet is able to survive the migration when  $e_{\max} > e_{\text{dis}}$ , being partially stripped).

If migration due to ZLK oscillations is successful, the final semimajor axis of the BD can be approximated as

$$a_{\text{BD,f}} \approx 2a_{\text{BD,0}}(1 - e_{\max}), \quad (8)$$

where subscripts f and 0 stand for after and before migration, respectively. We found that when equation (8) is evaluated for solutions of equation (4) located in the migration window, the resulting range of final semimajor axis ( $0.0043 \text{ au} \lesssim a_{\text{BD,f}} \lesssim 0.0166 \text{ au}$ ) is  $\approx 1\sigma$  below the one derived using  $M_{\text{WD,inner}} = 0.52 \pm 0.02$ ,  $M_{\text{BD}} = 0.07 \pm 0.01$ , and the orbital separation calculated from the orbital period reported by Rebassa-Mansergas et al. (2022,  $0.0169 \pm 2.8 \times 10^{-4}$  au). This result is depicted in the zoomed portion of Fig. 2, in which the eccentricity required (according to equation 8, red dotted line) for the BD to reach the observed orbital period is always below the migration window. This rather small discrepancy can be solved either by assuming a slightly lower total mass for the WD/BD binary (especially a smaller BD mass than what we assumed cannot be excluded given the weak current observational constraints) or by assuming in our model a smaller outer semimajor axis, so the maximum inner eccentricity reaches the migration window at smaller inner semimajor axis where solutions of equation (8) also are in this window. An example of the latter is depicted by the green line in Fig. 2, which shows  $e_{\max}$  when  $a_{\text{outer}} = 1115$  au (this value is obtained if we assume  $e_{\text{outer}} = 0.5$  and the observed projected separation being

the outer apoapsis distance). In this configuration,  $e_{\max}$  reaches the migration window when  $a_{\text{BD}} \gtrsim 3.2$  au and the minimum eccentricity for migration is  $\approx 0.997$  with a similar range of mutual inclinations.

The results presented above suggest that ZLK oscillations are able to induce inward migration although two main conditions are required to make this possible. One needs (1) the inner eccentricity to be at least  $\approx 0.997$  that in turn implies that (2) the mutual orbital inclination should be between  $\approx 86^\circ$  and  $\approx 94^\circ$ .

### 3.2 Validity of the analytical model used

The analytical model used by Muñoz & Petrovich (2020), developed to find the parameter space in which the tight orbit of the planet candidate in WD 1856 can be explained by tidal migration due to ZLK oscillations, concluded that such configuration is only reproduced if the initial (i.e. during the main-sequence stage of the host and tertiary) semimajor axis of the planet is located within a narrow range of values. This result, however, is in disagreement with the outcome of the numerical simulations performed by Stephan et al. (2021), who derived a much wider range of initial semimajor axis. As discussed by Stephan et al. (2021), this discrepancy can be explained considering the following two differences in the modelling: (1) The analytical condition imposed by Muñoz & Petrovich (2020) for the planet to survive the evolution of its host is much more restrictive than the numerical simulations performed by Stephan et al. (2021). (2) Unlike Muñoz & Petrovich (2020), Stephan et al. (2021) consider the scenario in which the planet crosses the Roche limit (i.e. the planet reaches eccentricities above  $e_{\text{dis}}$ ) and is partially stripped by tidal forces but survives the migration process.

Because of these limitations of the analytical prescriptions from Muñoz & Petrovich (2020), in our analysis we simply assumed that the BD survived the evolution of its host and emphasize only the minimum eccentricity required to achieve migration. In addition, unlike Muñoz & Petrovich (2020) we treated the outer semimajor axis as a free parameter. In this regard, it is important to recall that the outer semimajor axis used in Section 3.1 serves as an example and does not exclude configurations with smaller (larger) values, which will move the maximum eccentricity attained by the BD towards smaller (larger) inner semimajor axis. For instance, taking  $a_{\text{outer}} = 2500$  au the minimum eccentricity for migration is  $\approx 0.9989$  at  $a_{\text{BD}} \approx 7$  au as shown by the brown line in Fig. 2.

This result is consistent with the findings of Stephan et al. (2021) on WD 1856, which has a very similar configuration. The range of initial semimajor axis Stephan et al. (2021) derived for the planet orbiting WD 1856 peaks close to 100 au. At such distances,  $\xi_{\text{tide}}$  and  $\xi_{\text{GR}}$  become negligible and the maximum eccentricity only depends on the mutual inclination  $i$  between the inner and outer orbits  $\{e_{\max} = [1 - 5\cos^2(i)/3]^{1/2}\}$ . According to equation (8), and neglecting any orbital expansion due to stellar evolution mass-loss,<sup>3</sup> a BD/planet located at 100 au from its host star/WD would require an eccentricity of  $\approx 0.9999$  to migrate to 0.02 au, which in turn would require  $i \approx 89.4^\circ$ .

<sup>3</sup>This assumption provides a lower limit on the true eccentricity required for migration. If the orbit expands adiabatically (i.e. the orbital separation increases by a factor  $M_{\text{tot,0}}/M_{\text{tot,f}}$ , where  $M_{\text{tot}}$  is the total mass of the inner binary and subscripts f and 0 stand for after and before mass-loss), the BD/planet semimajor axis would increase by a factor of  $\approx 1.9$  after the formation of the host WD.

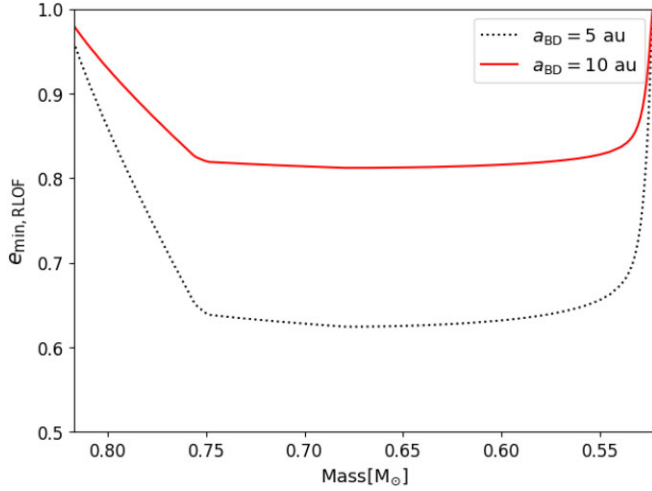


**Figure 3.** Minimum eccentricity required for RLOF (equation 9) as function of the mass of the inner WD progenitor during the AGB from the SSE model. For a BD semimajor axis equal to 5 au (10 au), the minimum eccentricity is  $\approx 0.62$  ( $\approx 0.81$ ) when the host star has a mass of  $\approx 0.67 M_{\odot}$  on the thermally pulsating AGB.

### 3.3 Migration scenario due to ZLK oscillations coupled with common envelope evolution

Even if ZLK oscillations did not produce eccentricities high enough for tidal migration, lower values of the eccentricity could still have impacted the evolution and perhaps triggered common envelope evolution, similar to what has been proposed for the transiting planet around WD 1856+534 (e.g. Lagos et al. 2021; Trani et al. 2022).

In order to estimate the minimum eccentricity required to start Roche lobe overflow (RLOF), we use the Roche lobe radius approximation for eccentric orbits given by Sepinsky, Willems & Kalogera (2007, their equation 45) evaluated at the periastris of the binary and taking the Roche radius equal to the stellar radius  $R_{\star}$  at the onset of mass transfer:

$$e_{\min, \text{RLOF}} = 1 - \frac{R_{\star}}{a_{\text{BD}}} \frac{0.6q^{2/3} + \ln(1 + q^{1/3})}{0.49q^{2/3}}. \quad (9)$$

Here,  $q = M_{\star}/M_{\text{BD}}$  is the mass ratio between the host star and the BD. Both  $R_{\star}$  and  $M_{\star}$  are obtained from SSE. Fig. 3 shows that for a separation of 5 (10) au, the eccentricity required to trigger mass transfer is  $e_{\min, \text{RLOF}} \approx 0.62$  ( $\approx 0.81$ ) when the host star has a mass of  $\approx 0.67 M_{\odot}$  during the AGB phase.

To provide one exemplary full simulation of the outlined triple star evolution, we used the MULTIPLE STELLAR EVOLUTION<sup>4</sup> (MSE;

<sup>4</sup><https://github.com/hamers/mse>. MSE is based on the SSE (Hurley et al. 2000) and binary stellar evolution (BSE; Hurley, Tout & Pols 2002) codes.

Hamers et al. 2021) code version 0.86, which allows to calculate the secular orbital evolution of the BD including the effects of stellar and tidal evolution, general relativity,  $N$ -body dynamics, and binary interactions. Table 2 summarizes the initial parameters used in our simulation. After  $\approx 2$  Gyr, the tertiary star evolves into a WD and its orbit expands, increasing the time-scale of the ZLK oscillations but keeping approximately the same maximum eccentricity (Fig. 4). When the host star evolves through the AGB, the inner eccentricity is still high enough ( $e \approx 0.73$ ) to trigger RLOF. Although this simulation assumes an outer semimajor axis of  $\approx 700$  au (which according to the adiabatic mass-loss model will increase to the observed projected separation of  $\sim 1700$  au), we verified with additional simulations that for an initial outer semimajor axis up to 1200 au ZLK oscillations with tidal friction are still able to lead to RLOF during the AGB. It therefore appears to be possible that the ZLK mechanism played a role in the evolution of the triple system prior to common envelope evolution.

## 4 CONCLUSION

We have studied in detail the evolutionary history of the WD + BD binary Gaia 0007–1605, which is the inner binary of a hierarchical triple star system with the tertiary being a WD that is  $\approx 8$  Gyr older than the inner one. We found that assuming the planet survived the evolution of its host star into a WD, ZLK oscillations alone can explain the configuration we observe today if the inner eccentricity reached values close or above  $\approx 0.997$ , which in turn implies that the inner and outer orbits were (or are) close to being perpendicular to each other.

By reconstructing through common envelope evolution the close orbit of the BD we observe today, we found that no energy in addition to orbital energy is required to understand the currently observed period. Our findings further support the conclusions recently drawn by Zorotovic & Schreiber (2022) that, in contrast to previous findings (e.g. De Marco et al. 2011), common envelope evolution with substellar companions does not require additional energy sources to play a role. This also further illustrates that in terms of the energy budget of common envelope evolution, the transiting planet around WD 1856+534 remains an outlier as additional energy is required to reproduce the currently observed period with common envelope evolution. The idea that an additional planet might have contributed to the ejection of the envelope (e.g. Bear & Soker 2011), as suggested first by Lagos et al. (2021) and later investigated in more detail by Chamandy et al. (2021), offers an elegant solution for this particular system (although it will be impossible to verify this hypothesis).

However, when considering constraints on common envelope evolution from WD + BD binaries it is important to keep in mind that Gaia 0007–1605 and WD 1856+534 might not be post common envelope systems, i.e. both common envelope evolution and/or ZLK oscillations plus tidal migration appear as potential scenarios to have produced the currently observed configuration.

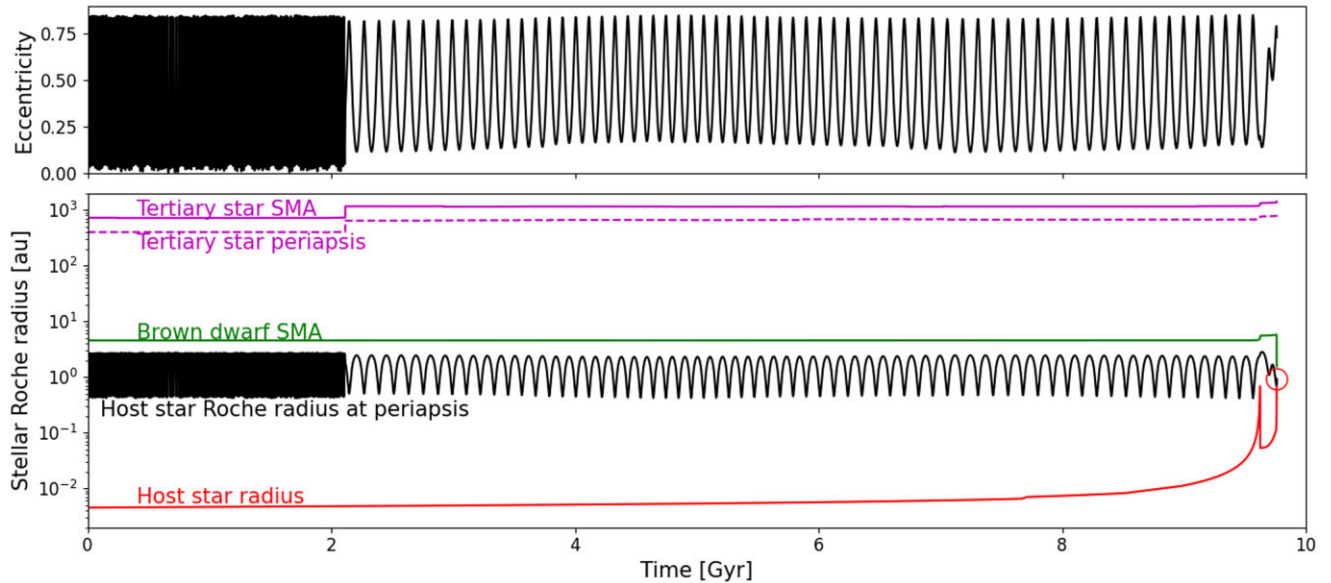


**Figure 4.** Orbital evolution of Gaia 0007–1605 according to the initial orbital configuration given in Table 2. The simulation is stopped when RLOF starts in the inner binary (red circle). **Top panel:** Evolution of the BD eccentricity. While the host and tertiary stars are on the main-sequence ( $\lesssim 2$  Gyr) ZLK oscillations produce a maximum inner eccentricity of  $\approx 0.85$ . After  $\approx 2$  Gyr, the tertiary star evolves into a WD, its semimajor axis increases and therefore also the time-scale of the ZLK oscillations. **Bottom panel:** Evolution of the tertiary star semimajor axis and periapsis (solid and dashed magenta lines, respectively), BD semimajor axis (green line), and stellar radius and Roche radius at periapsis of the host star (red and black lines, respectively). At  $\approx 9.7$  Gyr, the eccentricity of the inner binary is high enough ( $\approx 0.73$ ) to trigger RLOF (denoted by the red circle) when the semimajor axis of the BD and the tertiary star are  $\approx 1.5$  au (orbital period of  $\approx 720$  d) and  $\approx 1400$  au, respectively.

**Table 2.** Configuration assumed for Gaia 0007–1605 at the beginning of the MSE simulation. Stellar radii and apsidal motion constants ( $k_{AM}$ ) are set internally by the code. For the BD, we use  $R_{BD} = 0.086 R_{\odot}$  (expressed in au) and  $k_{AM} = 0.143$  (i.e. half of the Love number of degree 2). The number of output steps is set to 20 000. The mutual inclination between the inner and outer orbits is  $65.8^{\circ}$ .

Parameter	Host star	Tertiary star	Brown dwarf
Mass ( $M_{\odot}$ )	1.07	1.7	0.07
Radius (au)	Default	Default	$4 \times 10^{-3}$
Metallicity	Solar	Solar	Solar
Apsidal motion constant	0.19	0.19	0.143
Orbital parameter	Inner orbit	Outer orbit	–
Eccentricity	0	0.45	–
Semimajor axis (au)	4.5	720	–
Inclination (rad)	0.001	1.15	–
Argument of pericentre (rad)	0.01	0.5	–
Longitude of ascending node (rad)	0.5	0.5	–

## ACKNOWLEDGEMENTS

We thank the referee for helpful comments and suggestions. This project has received funding from the European Research Council (ERC) under the European Union’s Horizon 2020 Research and Innovation Programme (grant agreement no. 101020057). MRS and MZ acknowledge support from Fondo Nacional de Desarrollo Científico y Tecnológico (FONDECYT, grant no. 1221059). MRS also acknowledges support by the Agencia Nacional de Investigación y Desarrollo (ANID) – Millennium Science Initiative Program – NCN19\_171. This research was supported in part by the National Science Foundation under grant no. NSF PHY-1748958.

## DATA AVAILABILITY

The data and numerical tools used in this article can be obtained upon request to the corresponding author and after agreeing to the terms of use.

## REFERENCES

- Alonso R. et al., 2021, *A&A*, 649, A131  
 Baraffe I., Chabrier G., Barman T. S., Allard F., Hauschildt P. H., 2003, *A&A*, 402, 701  
 Bear E., Soker N., 2011, *MNRAS*, 411, 1792  
 Chamandy L., Blackman E. G., Nordhaus J., Wilson E., 2021, *MNRAS*, 502, L110  
 De Marco O., Passy J.-C., Moe M., Herwig F., Mac Low M.-M., Paxton B., 2011, *MNRAS*, 411, 2277  
 El-Badry K., Rix H.-W., Heintz T. M., 2021, *MNRAS*, 506, 2269  
 Gentile Fusillo N. P. et al., 2021, *MNRAS*, 508, 3877  
 Guillochon J., Ramirez-Ruiz E., Lin D., 2011, *ApJ*, 732, 74  
 Hamers A. S., Rantala A., Neunteufel P., Preece H., Vynatheya P., 2021, *MNRAS*, 502, 4479  
 Heller R., Jackson B., Barnes R., Greenberg R., Homeier D., 2010, *A&A*, 514, A22  
 Hernandez M. S. et al., 2021, *MNRAS*, 501, 1677  
 Hernandez M. S. et al., 2022a, *MNRAS*, 512, 1843  
 Hernandez M. S. et al., 2022b, *MNRAS*, 517, 2867  
 Hurley J. R., Pols O. R., Tout C. A., 2000, *MNRAS*, 315, 543  
 Hurley J. R., Tout C. A., Pols O. R., 2002, *MNRAS*, 329, 897  
 Ivanova N. et al., 2013, *A&AR*, 21, 59  
 Kozai Y., 1962, *AJ*, 67, 591  
 Lagos F., Schreiber M. R., Zorotovic M., Gänsicke B. T., Ronco M. P., Hamers A. S., 2021, *MNRAS*, 501, 676

- Lagos F., Schreiber M. R., Parsons S. G., Toloza O., Gänsicke B. T., Hernandez M. S., Schmidtbreick L., Belloni D., 2022, *MNRAS*, 512, 2625
- Lidov M. L., 1962, *Planet. Space Sci.*, 9, 719
- Liu B., Muñoz D. J., Lai D., 2015, *MNRAS*, 447, 747
- Masuda K., Kawahara H., Latham D. W., Bieryla A., Kunitomo M., MacLeod M., Aoki W., 2019, *ApJ*, 881, L3
- Merlov A., Bear E., Soker N., 2021, *ApJ*, 915, L34
- Muñoz D. J., Petrovich C., 2020, *ApJ*, 904, L3
- Naoz S., 2016, *ARA&A*, 54, 441
- Naoz S., Farr W. M., Lithwick Y., Rasio F. A., Teyssandier J., 2011, *Nature*, 473, 187
- Nelemans G., Verbunt F., Yungelson L. R., Portegies Zwart S. F., 2000, *A&A*, 360, 1011
- O'Connor C. E., Liu B., Lai D., 2021, *MNRAS*, 501, 507
- Paczynski B., 1976, in Eggleton P., Mitton S., Whelan J., eds, Proc. IAU Symp. Vol. 73, Structure and Evolution of Close Binary Systems. 75, Reidel, Dordrecht.
- Perets H. B., Fabrycky D. C., 2009, *ApJ*, 697, 1048
- Petrovich C., 2015, *ApJ*, 799, 27
- Rebassa-Mansergas A. et al., 2021, *MNRAS*, 505, 3165
- Rebassa-Mansergas A., Xu S., Raddi R., Pala A. F., Solano E., Torres S., Jiménez-Esteban F., Cruz P., 2022, *ApJ*, 927, L31
- Schreiber M. R., Gänsicke B. T., 2003, *A&A*, 406, 305
- Sepinsky J. F., Willems B., Kalogera V., 2007, *ApJ*, 660, 1624
- Stephan A. P., Naoz S., Gaudi B. S., 2021, *ApJ*, 922, 4
- Thompson T. A., 2011, *ApJ*, 741, 82
- Trani A. A., Rieder S., Tanikawa A., Iorio G., Martini R., Karelín G., Glanz H., Portegies Zwart S., 2022, *Phys. Rev. D*, 106, 043014
- Vanderburg A. et al., 2020, *Nature*, 585, 363
- Von Zeipel H., 1910, *Astron. Nachr.*, 183, 345
- Webbink R. F., 1984, *ApJ*, 277, 355
- Webbink R. F., 2008, in Milone E. F., Leahy D. A., Hobill D. W., eds, *Astrophysics and Space Science Library*, Vol. 352, Short-Period Binary Stars: Observations, Analyses, and Results. Springer, Dordrecht, p. 233
- Woods T. E., Ivanova N., van der Sluys M. V., Chaichenets S., 2012, *ApJ*, 744, 12
- Wu Y., Murray N., 2003, *ApJ*, 589, 605
- Xu S. et al., 2021, *AJ*, 162, 296
- Zorotovic M., Schreiber M., 2022, *MNRAS*, 513, 3587
- Zorotovic M., Schreiber M. R., Gänsicke B. T., Nebot Gómez-Morán A., 2010, *A&A*, 520, A86

This paper has been typeset from a  $\text{\TeX}/\text{\LaTeX}$  file prepared by the author.